Recipient-biased competition for a cross-fed nutrient is required for coexistence of microbial mutualists

Running title: Biased competition within a mutualism

Alexandra L. McCully, Breah LaSarre, James B. McKinlay[#]

[#]Corresponding author. 1001 E 3rd Street, Jordan Hall, Bloomington, IN 47405

Phone: 812-855-0359

Email: jmckinla@indiana.edu

Conflict of interest.

The authors declare no conflict of interest.

Abstract. Many mutualistic microbial relationships are based on the exchange of nutrients, or cross-feeding. Traditionally, cross-feeding interactions are viewed as being unidirectional from the producer to the recipient. This is likely true when a cross-fed nutrient is a waste-product of the producer's metabolism. However, in some cases the nutrient holds value for both the producer and the recipient. In such cases, there is potential for reacquisition of a valuable cross-fed nutrient by producers in a population, essentially leading to competition against the recipients. The consequences of inter-partner competition for cross-fed nutrients on mutualism dynamics have not been considered. We investigated the effects of such competition on a mutualism using a synthetic anaerobic coculture pairing fermentative *Escherichia coli* and phototrophic *Rhodopseudomonas palustris*. In this coculture, *E. coli* excretes waste organic acids that serve as a carbon source for *R. palustris*. In return, *R.* palustris cross-feeds *E. coli* ammonium (NH_4^+), a valuable nitrogen source that both species in the mutualism prefer. To interrogate the impact of inter-partner competition, we varied the relative affinities for NH_4^+ in each species in coculture, both theoretically using kinetic model simulations and experimentally using mutants lacking NH_4^+ transporters. We demonstrated that the recipient partner must have a competitive advantage in acquiring a valuable cross-fed nutrient in order for the mutualism to persist. Our results reveal that inter-partner competition shaping mutualism dynamics is not limited to environmental resources but rather can apply to the very metabolites that form the basis of the cooperative relationship.

Significance. Mutualistic relationships, particularly those based on nutrient cross-feeding, play crucial roles in the stability of diverse ecosystems and drive global biogeochemical cycles. Cross-fed nutrients within these systems can be either waste products valued only by one partner or nutrients that both partners value. Here, we explore how inter-partner competition for a valuable cross-fed nutrient impacts mutualism dynamics. We discovered that mutualism stability necessitates that the recipient must be competitive in obtaining the cross-fed nutrient. We propose that the requirement for recipient-biased competition is a general rule for mutualistic coexistence based on the transfer of mutually valuable resources, microbial or otherwise.

Introduction

Mutualistic cross-feeding of resources between microbes can have important societal impacts ranging from affecting host health (1, 2) to driving global biogeochemical cycles (3–6). Cross-fed metabolites are often regarded as nutrients due to the value they provide to a dependent partner, hereon called the recipient. However, for the partner producing the nutrient, hereon called the producer, a cross-fed nutrient's value can vary. On one extreme, the cross-fed nutrient is valued by the recipient but holds no value for the producer, as is the case for fermentative waste products (7–10). In other cases, a cross-fed nutrient holds value for the producer, as is the case for vitamin B_{12} (6, 11, 12) and ammonium (NH_4^+) (13, 14), which a producer can usually use to support its own growth. Such valuable cross-fed nutrients are subject to partial privatization (15), wherein the producer has mechanisms to retain a portion of the nutrient pool for itself. We wondered whether these mechanisms for partial privatization could lead to competition between partner populations for a mutually valuable cross-fed nutrient. While competition within mutualisms for exogenous limiting resources has been recognized to influence mutualism stability (8, 16–19), most mutualism cross-feeding studies only consider unidirectional transfer from producer to recipient. To the best of our knowledge competition for valuable cross-fed nutrients between producer and recipient populations has never been addressed.

One prominent example of cross-feeding that could involve competition between mutualistic partners is NH_4^+ excretion by N_2-fixing bacteria (Fig. 1A), hereon called N_2-fixers (13, 14). During N_2 fixation, the enzyme nitrogenase converts N_2 gas into 2 NH_3 (20). In an aqueous environment, NH_3 is in equilibrium with NH_4^+. At neutral pH, NH_4^+ is the predominant form but small amounts of NH_3 can potentially leave the cell by diffusion across the membrane (21) (Fig. 1B). This extracellular NH_3 is then available to neighboring microbes, including clonal N_2-fixers, as NH_3/NH_4^+ is a preferred nitrogen source for most microbes. At concentrations above 20 μM, NH_3 can be acquired by passive diffusion; below 20 μM, NH_4^+ is bound and transported as NH_3 by AmtB transporters (Fig. 1B) (22). AmtB-like transporters are conserved throughout all domains of life (23). There is growing evidence that AmtB is used by N_2-fixers to recapture NH_3 lost by passive diffusion, as ΔAmtB mutants accumulate NH_4^+ in culture supernatants

64 (24–26). Thus, during the transfer of NH_4^+ from N_2-fixers to mutualistic partners, AmtB could allow
65 individual producer cells to compete against recipient cells for NH_4^+.
66 Assessing how competition between mutualistic partners for a cross-fed nutrient impacts a mutualism
67 would require a level of experimental control not found in most natural settings. However, synthetic
68 microbial communities, or cocultures, are well-suited to address such questions (27–29). We previously
69 developed a bacterial coculture wherein coexistence and coupled growth of two species is stabilized by
70 mutualistic cross-feeding (Fig. 1A) (26). In this coculture, *Escherichia coli* (*Ec*) ferments sugars into
71 waste organic acids, providing essential carbon and electrons to a genetically engineered
72 *Rhodopseudomonas palustris* (*Rp*) strain (Nx). In return *R. palustris* Nx excretes low micromolar
73 amounts of NH_4^+, providing essential nitrogen for *E. coli* (26). NH_4^+ excretion by *R. palustris* Nx is due to
74 the genetic deletion of the Q-linker region of NifA, the master transcriptional regulator of nitrogenase
75 (30). This mutation causes constitutive nitrogenase activity even in the presence of NH_4^+, a compound
76 that normally inhibits nitrogenase (31, 32). We previously established that net NH_4^+ excretion levels are
77 an important driver of coculture dynamics (26, 33). As NH_4^+ is a preferred nitrogen source for both *E. coli*
78 (the recipient) and *R. palustris* (the producer), the coculture is well suited to address how competition for
79 a cross-fed resource influences mutualism dynamics.
80 Here, we demonstrate that inter-partner competition for a cross-fed nutrient, NH_4^+, plays a direct role
81 in maintaining coexistence. Using both kinetic modeling and genetic manipulation, we determined that
82 successful coexistence of mutualistic partners depends on their relative affinities for NH_4^+. Insufficient
83 competition by *E. coli* for NH_4^+ resulted in a collapse of the mutualism. Mutualism collapse could be
84 delayed or potentially avoided through higher net NH_4^+ excretion by *R. palustris* or increased *E. coli*
85 population size. As a general rule, competition for a cross-fed nutrient in an obligate mutualism must be
86 biased in favor of the recipient to avoid extinction of both partner populations.

Results

Competition for cross-fed NH_4^+ is predicted to shape mutualism population dynamics. Our coculture features cross-feeding of both waste products and a mutually valuable nutrient (Fig 1A). Cross-fed organic acids are excreted as an *E. coli* waste product and are thus only useful to *R. palustris*. In contrast, NH_4^+ fixed by *R. palustris* Nx is essential for growth of both species in coculture; *R. palustris* uses a portion of the NH_4^+ for its own biosynthesis and excretes NH_4^+ for use as a nitrogen source by *E. coli.* However, *R. palustris* prefers NH_4^+ as a nitrogen source for growth (31), thus it is possible that individuals within the *R. palustris* Nx population also take up and assimilate excreted NH_4^+. We hypothesized that competition for NH_4^+ between *R. palustris* producer and *E. coli* recipient populations could skew species ratios and potentially disrupt mutualism stability. To test whether competition for cross-fed NH_4^+ could affect mutualism population dynamics we first used a mathematical model describing our coculture, SyFFoN (26, 33). SyFFoN simulates population and metabolic trends in batch cocultures using Monod model equations with experimentally-determined parameter values. Previous versions described NH_4^+ uptake kinetics for *E. coli* but not for *R. palustris* (26, 33). We therefore amended SyFFoN to include an *R. palustris* uptake affinity (K_M) for NH_4^+ and higher *R. palustris* maximum growth rate (μ_{MAX}) when NH_4^+ is used (Supplementary Table 1). We then simulated batch cocultures wherein the two species have different relative affinities for NH_4^+ (Fig. 2). The model predicted that when the *R. palustris* affinity for NH_4^+ is low relative to that of *E. coli* (*Rp*:*Ec* < 1), there is coexistence as enough N_2 is converted to NH_4^+ to support *R. palustris* growth and enough NH_4^+ is excreted to support *E. coli* growth. However, when the *R. palustris* affinity for NH_4^+ is high relative to that of *E. coli* (*Rp*:*Ec* > 1), *E. coli* growth is no longer supported, likely because *E. coli* cannot compete for excreted NH_4^+. Even when the model predicted no *E. coli* growth, high *R. palustris* cell densities were predicted (Fig. 2). These high *R. palustris* densities occurred because the model allows for persistent low levels of organic acid cross-feeding stemming from *E. coli* maintenance metabolism even when *E. coli* is not growing (33).

113 **Genetic disruption of AmtB NH_4^+ transporters affects mutualistic partner frequencies.** Bacterial
114 cells are known to generally acquire NH_4^+ through two mechanisms: passive diffusion of NH_3 or uptake
115 by transporters called AmtB (Fig. 1A). We hypothesized that genetic disruption of AmtB activity in either
116 species would result in a lower affinity for NH_4^+ in that species and thus allow us to test how relative
117 affinity for NH_4^+ impacts coculture dynamics. We generated ΔAmtB mutants of both *E. coli* and *R.*
118 *palustris* and first characterized the impact of the mutations in monoculture. In monocultures with excess
119 NH_4Cl (15 mM), *E. coli* ΔAmtB grew at an equivalent growth rate and produced an identical
120 fermentation profile as wild-type (WT) *E. coli* (Supplementary Fig. 1). Our observations are consistent
121 with those previously made with *E. coli* ΔAmtB mutants where growth defects were only apparent at
122 NH_4^+ concentrations below 20 μM (22). In *R. palustris* monocultures with N_2 as the nitrogen source, *R.*
123 *palustris* ΔAmtB growth trends were equivalent to those of the parent strain; however, *R. palustris*
124 ΔAmtB excreted more NH_4^+ than the parent strain and about a third of that excreted by *R. palustris* Nx
125 (Supplementary Fig. 1C and D). NH_4^+ excretion by *R. palustris* ΔAmtB could be due to a decreased
126 ability to reacquire NH_4^+ lost by diffusion, resulting in increased net NH_4^+ excretion overall.
127 Alternatively, we considered that NH_4^+ excretion by *R. palustris* ΔAmtB could be due to improper
128 regulation of nitrogenase. Proper regulation of nitrogenase requires AmtB in several N_2-fixers, for
129 example to induce post-translational inhibition, or switch-off, of nitrogenase in response to NH_4^+ (25, 34).
130 We tested whether *R. palustris* ΔAmtB exhibits NH_4^+-induced switch-off of nitrogenase by adding NH_4Cl
131 to exponentially growing cultures and measuring H_2 production, an obligate product of the nitrogenase
132 reaction (35), as a proxy for nitrogenase activity. Upon NH_4Cl addition, H_2 production stopped in *R.*
133 *palustris* ΔAmtB cultures. In contrast, it only slowed slightly in *R. palustris* Nx cultures (Supplementary
134 Fig. 2), consistent with previous observations that strains with NifA* are incompetent for NH_4^+-induced
135 switch-off (31, 32). Like the parent strain, *R. palustris* ΔAmtB did not produce H_2 when grown with
136 NH_4^+, unlike *R. palustris* Nx (Supplementary Fig. 3). These observations demonstrate that *R. palustris*
137 ΔAmtB is competent for NH_4^+-induced nitrogenase shut-off and indicate that NH_4^+ excretion by *R.*
138 *palustris* ΔAmtB is due to a poor ability to reacquire NH_4^+ lost by diffusion.

139 We then compared the growth trends of cocultures containing either WT *E. coli* or *E. coli*
140 ΔAmtB, paired with either *R. palustris* ΔAmtB, *R. palustris* Nx, or *R. palustris* NxΔAmtB, the latter of
141 which we previously determined to exhibit 3-fold higher NH_4^+-excretion levels than the Nx strain in
142 monoculture (26). For each *R. palustris* partner, cocultures with *E. coli* ΔAmtB grew slower than
143 cocultures with WT *E. coli* (Fig. 3A,B). *E. coli* ΔAmtB also constituted a lower percentage of the
144 population and achieved lower cell densities compared to WT *E. coli* when paired with the same *R.*
145 *palustris* strain (Fig. 3C). These lower frequencies suggest that *E. coli* ΔAmtB was less competitive for
146 excreted NH_4^+ against *R. palustris*.
147 Consistent with previous work, *R. palustris* NxΔAmtB supported higher percentages and cell
148 densities of WT *E. coli* (Fig. 3C) due to a high level of NH_4^+ excretion (Supplementary Fig. 1D) (26). At
149 high NH_4^+ excretion levels from *R. palustris* NxΔAmtB, faster *E. coli* growth leads to rapid organic acid
150 accumulation, which acidifies the environment, inhibits *R. palustris* growth, and leaves organic acids
151 unconsumed (26) (Fig. 3D). Surprisingly, although *R. palustris* ΔAmtB excreted less NH_4^+ than *R.*
152 *palustris* Nx in monoculture, *R. palustris* ΔAmtB supported a higher WT *E. coli* population in coculture
153 and unconsumed organic acids remained after cessation of growth (Fig. 3C, D). Unlike Nx strains, which
154 have constitutive nitrogenase activity due to a mutation in the transcriptional activator NifA (30), *R.*
155 *palustris* ΔAmtB has a WT copy of NifA. Thus, *R. palustris* ΔAmtB can likely still regulate nitrogenase
156 expression, and thereby its activity, in response to nitrogen starvation. We hypothesized that *R. palustris*
157 ΔAmtB experiences a degree of nitrogen starvation when cocultured with WT *E. coli* but not when in
158 monoculture. In coculture, WT *E. coli* would consume the excreted NH_4^+ and thereby limit reacquisition
159 of NH_4^+ by *R. palustris* ΔAmtB; in an *R. palustris* ΔAmtB monoculture any lost NH_4^+ would remain
160 available to *R. palustris*. To test whether coculture conditions stimulated higher nitrogenase activity, we
161 quantified nitrogenase activity in both monocultures and cocultures using an acetylene reduction assay. In
162 agreement with our hypothesis, we found that *R. palustris* ΔAmtB had increased nitrogenase activity in
163 coculture conditions compared to monocultures whereas *R. palustris* Nx, which exhibits constitutive
164 nitrogenase activity, showed similar levels in both conditions (Supplementary Fig. 4). As *R. palustris*

165 ΔAmtB lacks an ammonium transporter, allowing WT *E. coli* to outcompete *R. palustris* for excreted
166 NH_4^+, the relatively high WT *E. coli* population in coculture with *R. palustris* ΔAmtB is likely supported
167 by both higher NH_4^+ cross-feeding due to increased nitrogenase activity and decreased *R. palustris*
168 affinity for NH_4^+.

169 ***E. coli* must have a competitive advantage for NH_4^+ acquisition to avoid extinction of both partners.**
170 Our coculture has been shown to support reproducible trends in response to both environmental and
171 genetic perturbations, including limiting NH_4^+ cross-feeding (26, 33). We were therefore surprised to
172 observe that cocultures of *R. palustris* ΔAmtB paired with *E. coli* ΔAmtB showed little growth when
173 started from a single colony of each species (Fig. 3), a method that we routinely use to initiate cocultures
174 (26, 33). We hypothesized that when both species lack AmtB, *R. palustris* might have a greater affinity
175 for NH_4^+ than *E. coli*, thereby preventing *E. coli* growth as predicted in our simulations (Fig. 2). Even
176 though our simulations predicted *R. palustris* growth when it outcompetes *E. coli* for NH_4^+ (Fig. 2),
177 SyFFoN likely underestimates the time required to achieve these densities, if they would be achieved at
178 all, as SyFFoN does not take into account cell death, which is known to occur when *E. coli* growth is
179 prevented in coculture (33).

180 We reasoned that if *E. coli* ΔAmtB was being outcompeted by *R. palustris* ΔAmtB for excreted
181 NH_4^+, then starting with a larger *E. coli* ΔAmtB population would increase the probability that any given
182 *E. coli* cell would acquire NH_4^+ versus *R. palustris*. To test this hypothesis we simulated batch cultures
183 with different starting species ratios and setting the *R. palustris* affinity for NH_4^+ to be far higher than that
184 of *E. coli* (*Rp:Ec* = 1000). The model predicted that when *E. coli* was inoculated at equal or higher
185 densities than *R. palustris*, the coculture would grow more (Fig. 4A). We tested this prediction
186 experimentally using cocultures of *R. palustris* ΔAmtB paired with *E. coli* ΔAmtB started at different cell
187 densities. Greater coculture growth was observed when cocultures were inoculated with equal or higher
188 relative densities of *E. coli* ΔAmtB versus *R. palustris* ΔAmtB (Fig. 4B, C). These data together suggest
189 that poor coculture growth is due to *E. coli* ΔAmtB having a lower NH_4^+ affinity than *R. palustris*
190 ΔAmtB.

191 We then sought to experimentally verify that *E. coli* ΔAmtB strains are less competitive against
192 *R. palustris* for NH_4^+ acquisition, even when *R. palustris* lacks AmtB. To determine relative NH_4^+
193 affinities, we directly competed all possible *E. coli* and *R. palustris* strain combinations in cocultures
194 where ample carbon was available for each species but the NH_4^+ concentration was kept low; specifically,
195 a small amount of NH_4^+ was added every hour to bring the final NH_4^+ concentration to 0.5 μM (Fig. 5). In
196 this competition assay, the species that is more competitive for NH_4^+ should reach a higher cell density
197 than the other species. In all cases, WT *E. coli* was more competitive for NH_4^+ than *R. palustris*.
198 However, each *R. palustris* strain was able to outcompete *E. coli* ΔAmtB (Fig. 5), even though the *R.*
199 *palustris* maximum growth rate is 4.6-times slower than that of *E. coli* (Supplementary Fig. 1). Even *R.*
200 *palustris* strains lacking AmtB outcompeted *E. coli* ΔAmtB (Fig. 5), suggesting that *R. palustris* has a
201 higher affinity for NH_4^+ than *E. coli* in the absence of AmtB. Thus, an inability of *E. coli* to compete
202 against *R. palustris* for cross-fed NH_4^+ likely explains why cocultures failed to grow when both partner
203 populations lacked AmtB (Fig. 3).
204 The collapse of cocultures pairing *R. palustris* ΔAmtB with *E. coli* ΔAmtB made us question why
205 cocultures pairing *R. palustris* Nx with *E. coli* ΔAmtB did not collapse (Fig. 3), since *R. palustris* Nx
206 possesses a functional AmtB and outcompeted *E. coli* ΔAmtB for NH_4^+ to a similar degree as in other
207 pairings with *E. coli* ΔAmtB (Fig. 5). We hypothesized that a relatively high NH_4^+ excretion level by *R.*
208 *palustris* Nx could compensate for a low *E. coli* NH_4^+ affinity (Supplementary Fig. 1D). We therefore
209 simulated cocultures with the *R. palustris* affinity for NH_4^+ set high relative to that of *E. coli* (*Rp*:*Ec* =
210 1000) and varied the *R. palustris* NH_4^+ excretion level (Fig. 6). Indeed, increasing *R. palustris* NH_4^+
211 excretion was predicted to overcome a low *E. coli* affinity for NH_4^+ and support growth of both species
212 (Fig. 6). However, at the highest levels of NH_4^+ excretion, *R. palustris* growth was predicted to be
213 inhibited due to rapid *E. coli* growth and subsequent production of organic acids that acidify the
214 environment (Fig. 6) (26). These simulations suggest that *R. palustris* Nx, and likely NxΔAmtB as well,
215 supported coculture growth with *E. coli* ΔAmtB due to higher NH_4^+ excretion levels (Supplementary Fig.

216 1D), whereas a combination of low NH_4^+ excretion by *R. palustris* ΔAmtB (Supplementary Fig. 1D) and
217 a low affinity for NH_4^+ by *E. coli* ΔAmtB led to collapse of the mutualism in this pairing.
218 So far, we had only considered the effect of severe discrepancies in NH_4^+ affinities between the two
219 species (e.g., 1000-fold difference in K_M values in our simulations) as a mechanism leading to coculture
220 collapse within the time period of a single culturing. However, we wondered if a subtle discrepancy in
221 NH_4^+ affinities could lead to coculture collapse if given more time. The lack of growth in cocultures with
222 *R. palustris* ΔAmtB paired with *E. coli* ΔAmtB made us question if other cocultures containing *E. coli*
223 ΔAmtB were truly stable or not. We therefore simulated serial transfers of cocultures with partners having
224 different relative NH_4^+ affinities (Fig. 7A, B). At equivalent NH_4^+ affinities (Fig. 7A), both species were
225 predicted to be maintained over serial transfers. However, when the relative affinities approached a
226 threshold (relative *Rp*:*Ec* = 2.75), cell densities of both species were predicted to decrease over serial
227 transfers (Fig. 7B). This decline in coculture growth is due to *E. coli* being slowly but progressively
228 outcompeted for NH_4^+ by *R. palustris*. As the difference between the *R. palustris* and *E. coli* populations
229 expands, *R. palustris* cells have a greater chance of acquiring NH_4^+ than the smaller *E. coli* population,
230 further starving *E. coli* for NH_4^+ and simultaneously cutting off *R. palustris* from its supply of organic
231 acids from *E. coli.*
232 The above prediction prompted us to investigate if cocultures pairing *R. palustris* with *E. coli*
233 ΔAmtB were stable through serial transfers. We focused on cocultures with *R. palustris* Nx rather than *R.*
234 *palustris* NxΔAmtB because *R. palustris* Nx has AmtB and would therefore be most likely to eventually
235 outcompete *E. coli* ΔAmtB. We serially transferred cocultures of *R. palustris* Nx paired with *E. coli*
236 ΔAmtB and monitored final cell densities. Strikingly, we observed coculture collapse after eight serial
237 transfers (Fig. 7C). This observation is in stark contrast to cocultures of *R. palustris* Nx paired with WT
238 *E. coli*, which we have serially transferred for over 100 transfers with no extinction events (unpublished
239 data). These results indicate that the recipient population must have a competitive advantage for a cross-
240 fed nutrient versus the producer population to avoid mutualism collapse and potential extinction of both
241 partner populations.

242 **Discussion**

243 Here we demonstrate that mutualistic partners can compete for a valuable cross-fed nutrient upon
244 which the mutualistic interaction is based, in this case NH_4^+. This competition can impact partner
245 frequencies and mutualism stability. Producer-biased competition for a cross-fed nutrient can render
246 nutrient excretion levels insufficient for cooperative growth, as efficient nutrient reacquisition by the
247 producer can starve the recipient, leading to tragedy of the commons (36). Conversely, recipient-biased
248 competition for a cross-fed nutrient drives cooperative directionality in nutrient exchange and thereby
249 promotes mutualism stability. One implication of these results is that inter-partner competition can
250 influence the level of resource privatization. Within microbial interdependencies, partial privatization has
251 primarily been thought to depend on mechanisms used by the producer to retain a portion of a mutually
252 valuable resource (15). Our data indicate that for excreted resources having a transient availability to both
253 mutualists, recipient acquisition mechanisms can also influence the level of privatization, as the
254 competition impacts how much of a cross-fed resource will be shared versus re-acquired. In effect,
255 recipient-biased competition avoids tragedy of the commons by enforcing partial privatization of a
256 mutually valuable resource. The importance of the recipient having the upper hand in inter-partner
257 competition likely applies to other synthetic cocultures and natural microbial mutualisms that are based
258 on the cross-feeding of valuable nutrients, including amino acids (37, 38) and vitamin B_{12} (6, 11). The
259 same rule could also apply to inter-kingdom and non-microbial examples of cross-feeding (plants and
260 pollinators, nutrient transfer between plants and bacteria or fungi (39)) and cooperative feeding (honey-
261 bird and human harvesting of bee hives (40), cooperative hunting between grouper fish and moray eels
262 (41)). In such cases, increased privatization of a cross-fed or shared resource, for example through
263 producer-biased competition, could threaten the mutualism upon which both species depend (15, 39, 42).

264 In our system, AmtB transporters were crucial determinants of inter-partner competition for NH_4^+.
265 We were intrigued to find that when both species lacked AmtB, *R. palustris* out-competed *E. coli* for
266 NH_4^+ (Fig. 5) enough so to collapse the mutualism within a single culturing (Fig. 3). Whether by
267 maximizing NH_4^+ retention or re-acquisition, *R. palustris*, and perhaps other N_2-fixers, might have

268 additional mechanisms aside from AmtB to minimize loss of NH_4^+ as NH_3. These mechanisms could
269 include a relatively low internal pH to favor NH_4^+ over NH_3, negatively-charged surface features, or
270 relatively high affinities by NH_4^+ assimilating enzymes such as glutamine synthetase. There are several
271 reasons why it would be beneficial for N_2-fixers to minimize NH_4^+ loss. First, N_2 fixation is expensive,
272 both in terms of the enzymes involved (43) and the reaction itself, costing 16 ATP to convert one N_2 into
273 2 NH_3 (35). Passive loss of NH_3 would only add to this cost, as more N_2 would have to be fixed to
274 compensate. Second, loss of NH_4^+ could benefit nearby microbes competing against an N_2-fixer for
275 separate limiting nutrients (14, 44). The possibility that N_2-fixers could have a superior ability to retain or
276 acquire NH_4^+ independently of AmtB is not farfetched. Bacteria are known to exhibit differential abilities
277 to compete for nutrients. For example, iron acquisition commonly involves iron-binding siderophores, but
278 siderophores can be chemically distinct and thereby differ in their affinity for iron (45). Strategies to
279 utilize siderophores as a shared resource are also numerous, leading to different cooperative or
280 competitive outcomes in microbial communities (45, 46). One must consider that additional mechanisms
281 for acquiring NH_4^+ beyond AmtB might likewise exist. As our results have raised the potential for inter-
282 partner competition for cross-fed resources themselves, understanding the physiological mechanisms that
283 confer competitive advantages between species will undoubtedly aid in describing the interplay between
284 competition and cooperation within mutualisms.
285

286 **Materials and Methods**

287 **Strains and growth conditions.** Strains, plasmids, and primers are listed in Supplementary Table 2. All
288 *R. palustris* strains contained *ΔuppE* and *ΔhupS* mutations to facilitate accurate colony forming unit
289 (CFU) measurements by preventing cell aggregation (49) and to prevent H_2 uptake, respectively. *E. coli*
290 was cultivated on Luria-Burtani (LB) agar and *R. palustris* on defined mineral (PM) (50) agar with 10
291 mM succinate. $(NH_4)_2SO_4$ was omitted from PM agar for determining *R. palustris* CFUs. Monocultures
292 and cocultures were grown in 10-mL of defined M9-derived coculture medium (MDC) (26) in 27-mL
293 anaerobic test tubes. To make the medium anaerobic, MDC was bubbled with N_2, and tubes were sealed

294 with rubber stoppers and aluminum crimps, and then autoclaved. After autoclaving, MDC was
295 supplemented with cation solution (1 % v/v; 100 mM $MgSO_4$ and 10 mM $CaCl_2$) and glucose (25 mM),
296 unless indicated otherwise. *E. coli* monocultures were also supplemented with 15mM NH_4Cl. All cultures
297 were grown at 30°C laying horizontally under a 60 W incandescent bulb with shaking at 150 rpm. Starter
298 cocultures were inoculated with 200 µL MDC containing a suspension of a single colony of each species.
299 Test cocultures were inoculated using a 1% inoculum from starter cocultures. Serial transfers were also
300 inoculated with a 1% inoculum. Kanamycin and gentamycin were added to a final concentration of 100
301 µg/ml for *R. palustris* and 15 µg/ml for *E. coli* where appropriate.
302 **Generation of *R. palustris* mutants.** *R. palustris* mutants were derived from wild-type CGA009 (51).
303 Generation of strains CGA4004, CGA4005, and CGA4021 was described previously (26). For generation
304 of strain CGA4026 (*R. palustris* ΔAmtB) the WT *nifA* gene was amplified using primers JBM1 and
305 JBM2, digested with XbaI and BamHI, and ligated into plasmid pJQ200SK to make pJQnifA16. This
306 suicide vector was then introduced into CGA4021 by conjugation, and sequential selection and screening
307 was performed as described (52) to replace *nifA** with WT *nifA*. Reintroduction of the WT *nifA* gene was
308 confirmed by PCR and sequencing.
309 **Generation of the *E. coli* ΔAmtB mutant.** P1 transduction (53) was used to introduce Δ*amtB::Km* from
310 the Keio collection strain JW0441-1 (54) into MG1655. The Δ*amtB::Km* genotype of kanamycin-resistant
311 colonies was confirmed by PCR and sequencing.
312 **Analytical procedures.** Cell density was assayed by optical density at 660 nm (OD_{660}) using a Genesys
313 20 visible spectrophotometer (Thermo-Fisher, Waltham, MA, USA). Growth curve readings were taken
314 in culture tubes without sampling (i.e., Tube OD_{660}). Specific growth rates were determined using
315 measurements between 0.1-1.0 OD_{660} where there is linear correlation between cell density and OD_{660}.
316 Final OD_{660} measurements were taken in cuvettes and samples were diluted into the linear range as
317 necessary. H_2 was quantified using a Shimadzu (Kyoto, Japan) gas chromatograph (GC) with a thermal
318 conductivity detector as described (55). Glucose, organic acids, formate and ethanol were quantified using

319 a Shimadzu high-performance liquid chromatograph (HPLC) as described (56). NH_4^+ was quantified
320 using an indophenol colorimetric assay as described (26).
321 **Nitrogenase activity.** Nitrogenase activity was measured using an acetylene reduction assay (43). Cells
322 from 10-mL cultures were harvested and resuspended in 10-mL fresh MDC medium in 27-mL sealed
323 tubes pre-flushed with argon gas. Suspensions were incubated in light for 1 hour at 30°C to recover.
324 Then, 250 µl of 100% acetylene gas was injected into the headspace to initiate the assay, and ethylene
325 production was measured over time by gas chromatography as described (43). Ethylene levels were
326 normalized to total *R. palustris* CFUs in the 10-ml volume.
327 **NH_4^+ competition assay.** Fed-batch cultures were performed in custom anaerobic serum vials with side
328 sampling ports. Each vial contained a stir bar and 30-mL of sterile, anaerobic MDC medium, and was
329 sealed at both ends with rubber stoppers and aluminum crimps. Each vial was supplemented with 25 mM
330 glucose, 1 % v/v cation solution and 20 mM sodium acetate. Starter monocultures of each species were
331 grown to equivalent CFUs/mL in MDC tubes containing limiting nutrients (3 mM sodium acetate for *R.*
332 *palustris* and 1.5 mM NH_4Cl for *E. coli*), and 1 mL of each species was inoculated into the serum vials.
333 These competition cocultures were incubated at 30°C under a 60 W incandescent bulb with constant
334 stirring at 200 rpm on a Variomag magnetic stirrer (Thermo Scientific) for 96 hours. NH_4Cl was fed to
335 cultures from a 500 µM NH_4Cl stock using a peristaltic pump (Watson-Marlow) on an automatic timer
336 (Intermatic DT620) at a rate of 0.33-mL/minute once an hour for 96 hours for a final concentration of ~
337 0.5 µM upon each addition. Each serum vial was constantly flushed with Ar gas to maintain anaerobic
338 conditions. Samples were taken at 0 and 96 h for quantification of CFUs.
339 **Mathematical modeling.** A Monod model describing bi-directional cross-feeding in batch cultures,
340 called SyFFoN_v3 (Syntrophy between Fermenter and Fixer of Nitrogen), was modified from our
341 previous model (33) to allow for competition between *E. coli* and *R. palustris* for NH_4^+ as follows: (i) an
342 equation for *R. palustris* growth rate on NH_4^+ was added to boost the *R. palustris* growth rate when
343 acquiring NH_4^+ and (ii) the Km of *R. palustris* for NH_4^+ (K_{AR}) was included. Equations and default

parameter values are in Supplementary Table 1. SyFFoN_v3 runs in R studio and is available for download at: https://github.com/McKinlab/Coculture-Mutualism.

Acknowledgments

We thank Richard Phillips (Indiana University) for providing equipment for the NH_4^+ competition assay. We also thank Jay Lennon (Indiana University) for helpful discussions on the manuscript. This work was supported in part by the U.S. Department of Energy, Office of Science, Office of Biological and Environmental Research, under Award Number DE-SC0008131, by the U.S. Army Research Office, grant W911NF-14-1-0411, and by the Indiana University College of Arts and Sciences.

References

1. Flint HJ, Duncan SH, Scott KP, Louis P (2007) Interactions and competition within the microbial community of the human colon: Links between diet and health: Minireview. Environ Microbiol 9(5):1101–1111.
2. Hammer ND, et al. (2014) Inter- and intraspecies metabolite exchange promotes virulence of antibiotic-resistant *Staphylococcus aureus*. Cell Host Microbe 16(4):531–537.
3. McInerney MJ, Sieber JR, Gunsalus RP (2010) Syntrophy in anaerobic global carbon cycles. Curr Opin Biotechnol 20(6):623–632.
4. Durham BP, et al. (2015) Cryptic carbon and sulfur cycling between surface ocean plankton. Proc Natl Acad Sci 112(2):453–457.
5. Reeburgh WS (2007) Oceanic methane biogeochemistry. Chem Rev 107:486–513.
6. Croft MT, Lawrence AD, Raux-Deery E, Warren MJ, Smith AG (2005) Algae acquire vitamin B12 through a symbiotic relationship with bacteria. Nature 438(7064):90–93.
7. McInerney MJ, et al. (2008) Physiology, ecology, phylogeny, and genomics of microorganisms capable of syntrophic metabolism. Ann N Y Acad Sci 1125:58–72.

369 8. Hillesland KL, Stahl D a (2010) Rapid evolution of stability and productivity at the origin of a
370 microbial mutualism. Proc Natl Acad Sci U S A 107(5):2124–2129.
371 9. Schink B (1997) Energetics of syntrophic cooperation in methanogenic degradation. Microbiol Mol
372 Biol Rev 61(2):262–280.
373 10. Stams AJM (1994) Metabolic interactions between anaerobic bacteria in methanogenic environments.
374 Antonie van Leeuwenhoek, 66(1–3):271–294.
375 11. Grant MA, Kazamia E, Cicuta P, Smith AG (2014) Direct exchange of vitamin B12 is demonstrated
376 by modelling the growth dynamics of algal-bacterial cocultures. ISME J 8(7):1–10.
377 12. Seth EC, Taga ME (2014) Nutrient cross-feeding in the microbial world. Front Microbiol 5(July):350.
378 13. Behrens S, et al. (2008) Linking microbial phylogeny to metabolic activity at the single-cell level by
379 using enhanced element labeling-catalyzed reporter deposition fluorescence in situ hybridization (EL-
380 FISH) and NanoSIMS. Appl Environ Microbiol 74(10):3143–3150.
381 14. Adam B, et al. (2015) N_2-fixation, ammonium release and N-transfer to the microbial and classical
382 food web within a plankton community. ISME J:1–10.
383 15. Estrela S, Morris JJ, Kerr B (2016) Private benefits and metabolic conflicts shape the emergence of
384 microbial interdependencies. Environ Microbiol 18(5):1415–1427.
385 16. Meyer JS, Tsuchiya HM (1975) Dynamics of mixed populations having complementary metabolism.
386 Biotechnol Bioeng 17:1065–1081.
387 17. Kim HJ, Boedicker JQ, Choi JW, Ismagilov RF (2008) Defined spatial structure stabilizes a synthetic
388 multispecies bacterial community. Proc Natl Acad Sci U S A 105(47):18188–18193.
389 18. Miura Y, Tanaka H, Okazaki M (1980) Stability analysis of commensal and mutual relations with
390 competitive assimilation in continuous mixed culture. Biotechnol Bioeng 22(5):929–946.
391 19. Estrela S, Trisos CH, Brown SP (2012) From metabolism to ecology: cross-feeding interactions shape
392 the balance between polymicrobial conflict and mutualism. Am Nat 180(5):566–576.

393 20. Bulen WA, LeComte JR (1966) The nitrogenase system from *Azotobacter*: two-enzyme requirement
394 for N_2 reduction, ATP-dependent H_2 evolution, and ATP hydrolysis. Proc Natl Acad Sci U S A
395 56(3):979–986.
396 21. Walter A, Gutknecht J (1986) Permeability of small nonelectrolytes through lipid bilayer membranes.
397 J Membr Biol 90(3):207–217.
398 22. Kim M, et al. (2012) Need-based activation of ammonium uptake in *Escherichia coli*. Mol Syst Biol
399 8(616):1–10.
400 23. Peng J, Huang CH (2006) Rh proteins vs Amt proteins: an organismal and phylogenetic perspective
401 on CO_2 and NH_3 gas channels. Transfus Clin Biol 13(1–2):85–94.
402 24. Barney BM, Eberhart LJ, Ohlert JM, Knutson CM, Plunkett MH (2015) Gene deletions resulting in
403 increased nitrogen release by *Azotobacter vinelandii*: Application of a novel nitrogen biosensor. Appl
404 Environ Microbiol 81(13):4316–4328.
405 25. Zhang T, et al. (2012) Involvement of the ammonium transporter AmtB in nitrogenase regulation and
406 ammonium excretion in *Pseudomonas stutzeri* A1501. Res Microbiol 163(5):332–339.
407 26. LaSarre B, McCully AL, Lennon JT, McKinlay JB (2017) Microbial mutualism dynamics governed
408 by dose-dependent toxicity of cross-fed nutrients. ISME J 11:337–348.
409 27. Widder S, et al. (2016) Challenges in microbial ecology: building predictive understanding of
410 community function and dynamics. ISME J 10:2557–2568.
411 28. Momeni B, Chen CC, Hillesland KL, Waite A, Shou W (2011) Using artificial systems to explore the
412 ecology and evolution of symbioses. Cell Mol Life Sci 68(8):1353–1368.
413 29. Lindemann SR, et al. (2016) Engineering microbial consortia for controllable outputs. ISME J
414 10:2077–2084.
415 30. McKinlay JB, Harwood CS (2010) Carbon dioxide fixation as a central redox cofactor recycling
416 mechanism in bacteria. Proc Natl Acad Sci U S A 107(26):11669–11675.
417 31. Rey FE, Heiniger EK, Harwood CS (2007) Redirection of metabolism for biological hydrogen
418 production. Appl Environ Microbiol 73(5):1665–1671.

419 32. Heiniger EK, Oda Y, Samanta SK, Harwood CS (2012) How posttranslational modification of
420 nitrogenase is circumvented in *Rhodopseudomonas palustris* strains that produce hydrogen gas
421 constitutively. Appl Environ Microbiol 78(4):1023–1032.
422 33. McCully AL, LaSarre B, McKinlay JB Growth-independent cross-feeding modifies boundaries for
423 coexistence in a bacterial mutualism. http://biorxiv.org/content/early/2016/10/25/083386
424 34. Yakunin AF, Hallenbeck PC (2002) AmtB is necessary for NH_4^+-induced nitrogenase switch-off and
425 ADP-ribosylation in *Rhodobacter capsulatus*. 184(15):4081–4088.
426 35. Hoffman BM, Lukoyanov D, Dean DR, Seefeldt LC (2013) Nitrogenase: A draft mechanism. Acc
427 Chem Res 46(2):587–595.
428 36. Rankin DJ, Bargum K, Kokko H (2007) The tragedy of the commons in evolutionary biology. Trends
429 Ecol Evol 22(12):643–651.
430 37. Pande S, et al. (2014) Fitness and stability of obligate cross-feeding interactions that emerge upon
431 gene loss in bacteria. ISME J 8(5):953–962.
432 38. Harcombe W (2010) Novel cooperation experimentally evolved between species. Evolution
433 64(7):2166–2172.
434 39. Bronstein JL (2001) The exploitation of mutualisms. Ecol Lett 4:277–287.
435 40. Isack HA, Reyer H-U (1989) Honeyguides and honey gatherers: Interspecific communication in a
436 symbiotic relationship. Science 243(4896):1343–1346.
437 41. Bshary R, Hohner A, Ait-el-Djoudi K, Fricke H (2006) Interspecific communicative and coordinated
438 hunting between groupers and giant moray eels in the red sea. PLoS Biol 4(12):2393–2398.
439 42. Sachs JL, Mueller UG, Wilcox TP, Bull JJ (2004) The evolution of cooperation. Q Rev Biol
440 51(2):211–244.
441 43. Oda Y, et al. (2005) Functional genomic analysis of three nitrogenase isozymes in the photosynthetic
442 bacterium *Rhodopseudomonas palustris*. J Bacteriol 187(22):7784–7794.
443 44. Morris JJ, Lenski RE, Zinser ER (2012) The black queen hypothesis: Evolution of dependencies
444 through adaptive gene loss. mBio 3(2):1–7.

445 45. Joshi F, Archana G, Desai A (2006) Siderophore cross-utilization amongst rhizospheric bacteria and
446 the role of their differential affinities for Fe^{3+} on growth stimulation under iron-limited conditions.
447 Curr Microbiol 53(2):141–147.
448 46. Niehus R, Picot A, Oliveira NM, Mitri S, Foster KR (2017) The evolution of siderophore production
449 as a competitive trait. Evolution (N Y). doi:10.1111/evo.13230.
450 47. Pande S, Kost C (2017) Bacterial unculturability and the formation of intercellular metabolic
451 networks. Trends Microbiol xx:1–13.
452 48. Blagodatskaya E, Littschwager J, Lauerer M, Kuzyakov Y (2014) Plant traits regulating N capture
453 define microbial competition in the rhizosphere. Eur J Soil Biol 61:41–48.
454 49. Fritts RK, Lasarre B, Stoner AM, Posto AL, McKinlay JB (2017) A *Rhizobiales*-specific unipolar
455 polysaccharide adhesin contributes to *Rhodopseudomonas palustris* biofilm formation across diverse
456 photoheterotrophic conditions. 83(4):1–14.
457 50. Kim M-K, Harwood CS (1991) Regulation of benzoate-CoA ligase in *Rhodopseudomonas palustris*.
458 FEMS Microbiol Lett 83:199–203.
459 51. Larimer FW, et al. (2004) Complete genome sequence of the metabolically versatile photosynthetic
460 bacterium *Rhodopseudomonas palustris*. Nat Biotechnol 22(1):55–61.
461 52. Rey FE, Oda Y, Harwood CS (2006) Regulation of uptake hydrogenase and effects of hydrogen
462 utilization on gene expression in *Rhodopseudomonas palustris*. J Bacteriol 188(17):6143–6152.
463 53. Thomason LC, Costantino N, Court DL (2007) *E. coli* genome manipulation by P1 transduction. Curr
464 Protoc Mol Biol doi: 10.1002/0471142727.mb0117s79.
465 54. Baba T, et al. (2006) Construction of *Escherichia coli* K-12 in-frame, single-gene knockout mutants:
466 the Keio collection. Mol Syst Biol 2:2006.0008.
467 55. Huang JJ, Heiniger EK, McKinlay JB, Harwood CS (2010) Production of hydrogen gas from light
468 and the inorganic electron donor thiosulfate by *Rhodopseudomonas palustris*. Appl Environ
469 Microbiol 76(23):7717–7722.

470 56. McKinlay JB, Zeikus JG, Vieille C (2005) Insights into *Actinobacillus succinogenes* fermentative
471 metabolism in a chemically defined growth medium. Appl Env Microbiol 71(11):6651–6656.
472 57. Buhr A, Daniels GA, Erni B (1992) The glucose transporter of *Escherichia coli*: Mutants with
473 impaired translocation activity that retain phosphorylation activity. J Biol Chem 267(6):3847–3851.
474 58. Khademi S, et al. (2004) Mechanism of ammonia transport by Amt/MEP/Rh: structure of AmtB at
475 1.35 A. Science 305(5690):1587–1594.
476 59. Hayashi K, et al. (2006) Highly accurate genome sequences of *Escherichia coli* K-12 strains MG1655
477 and W3110. Mol Syst Biol 2(1):2006.0007.

478

479 **Figures**

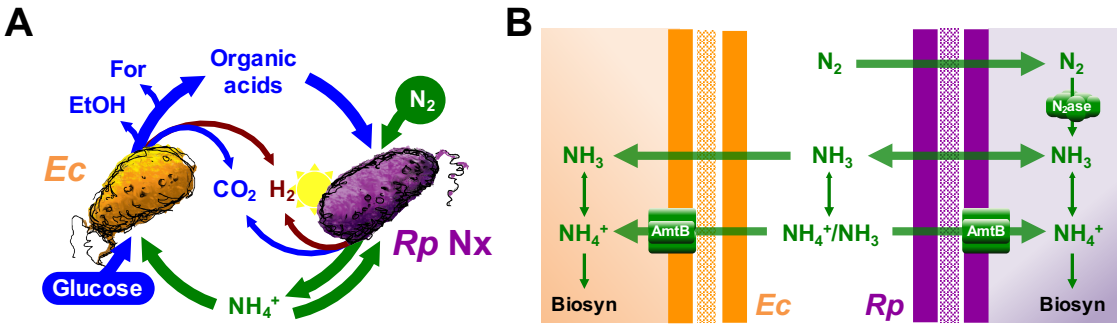

480

481 **Fig. 1. Mechanisms of NH_4^+ transfer within an obligate bacterial mutualism based on cross-feeding**
482 **of essential nutrients.** (**A**) *Escherichia coli* (*Ec*) anaerobically ferments glucose into organic acids,
483 supplying *Rhodopseudomonas palustris* Nx (*Rp* Nx) with essential carbon. *R. palustris* Nx fixes N_2 gas
484 and excretes NH_4^+, supplying *E. coli* with essential nitrogen. For, formate EtOH, ethanol. (**B**) NH_4^+ can be
485 passively lost from cells as NH_3. Both species encode high-affinity NH_4^+ transporters, AmtB, that
486 facilitate NH_4^+ uptake. NH_4^+ is the predominant form at neutral pH, as indicated by enlarged arrow head
487 on double-sided arrows.

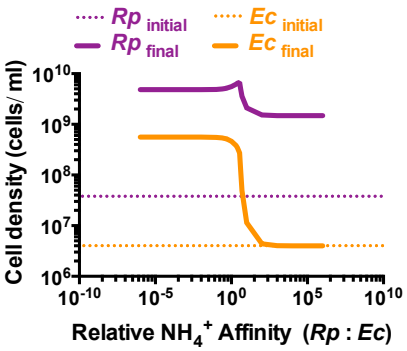

Fig. 2. Simulations suggest that *E. coli* must have a competitive advantage for NH_4^+ acquisition relative to *R. palustris* to support mutualistic growth. Final cell densities (solid lines) of *R. palustris* (*Rp*, purple) and *E. coli* (*Ec*, orange) after 300 h in simulated batch cultures for a range of relative NH_4^+ affinities. Initial cell densities are indicated by dotted lines. Relative NH_4^+ affinity values represent the relative *E. coli* K_M for NH_4^+ (K_A) compared to that of *R. palustris* (K_{AR}).

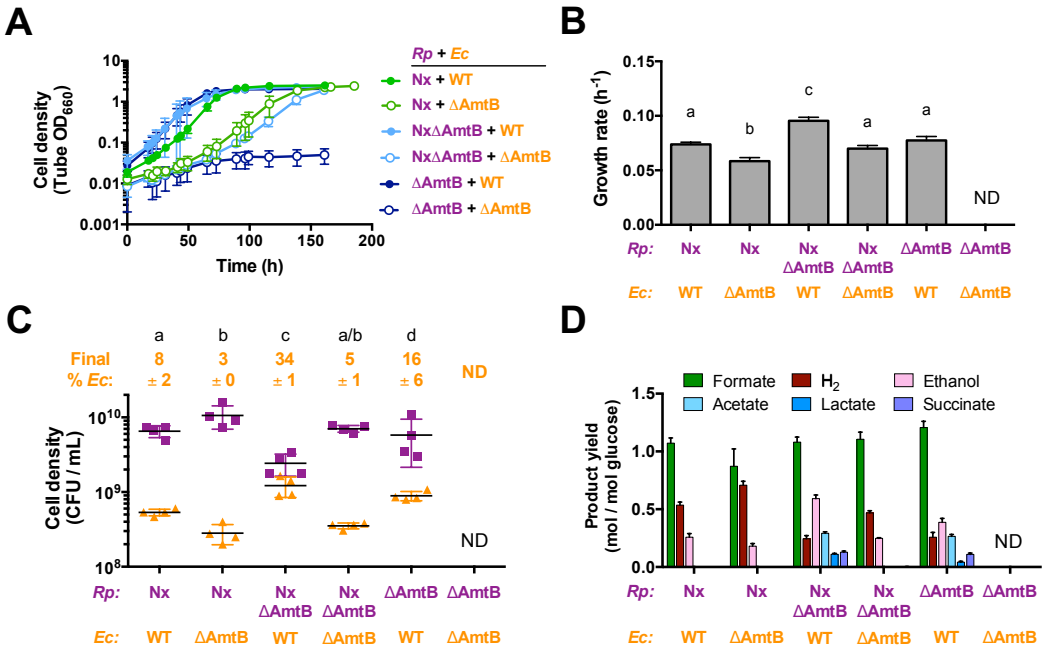

Fig. 3. NH_4^+ transporters influence population and metabolic trends of both partners in coculture. Growth curves (**A**), growth rates (**B**), final cell densities after one culturing (**C**), and fermentation product yields (**D**) from cocultures of all combinations of mutants lacking AmtB in each species. Final cell densities and fermentation product yields were taken after one week, within 24 hours into stationary

phase. ND, not determined. Error bars indicate SD, n=4. Different letters indicate statistical differences, $p < 0.05$, determined by one-way ANOVA with Tukey's multiple comparisons post test.

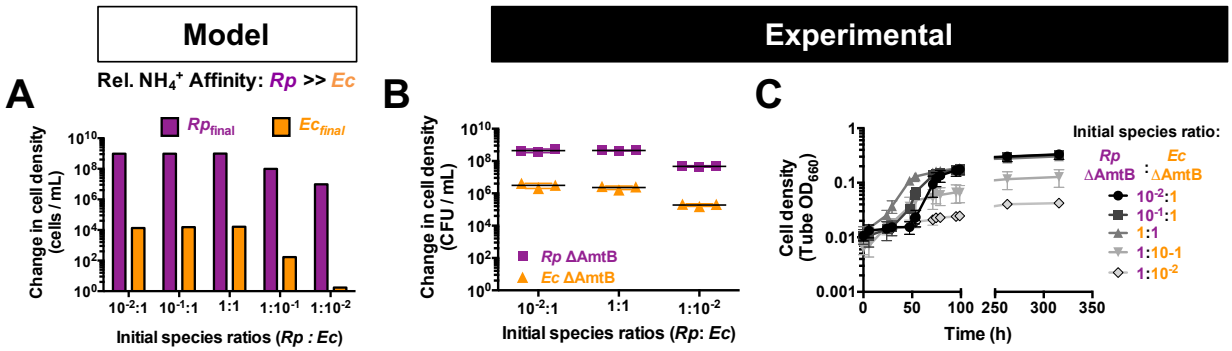

Fig. 4. Higher initial cell densities of *E. coli* ΔAmtB can partially compensate for a low *E. coli* NH_4^+ affinity. Simulations (**A**) and empirical data (**B**,**C**) showing the effect of initial *E. coli* (*Ec*) cell density on population and coculture growth trends when *E. coli* has a lower affinity for NH_4^+ compared to *R. palustris* (*Rp*). (**A**) 300 h batch cultures were simulated with a relative *R. palustris* : *E. coli* (*Rp* : *Ec*) K_M value for NH_4^+ of 0.001. (**B, C**) Change in cell densities after one week of growth (**B**) and growth curves (**C**) of cocultures inoculated at different species ratios. (**A-C**) A ratio value of 1 represents 2.7 x 10^6 CFUs/mL, which was experimentally measured from the starting inoculum for both species before diluting to achieve the indicated ratios. Error bars indicate SD, n=3.

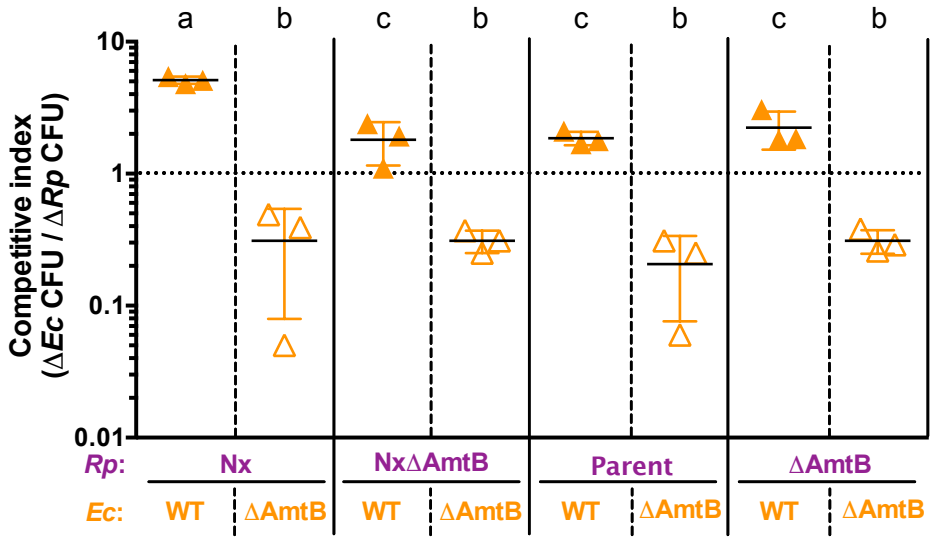

511

512 **Fig. 5. AmtB is important for competitive NH_4^+ acquisition.** Competitive indices for *E. coli* after 96
513 hours in NH_4^+-limited competition assay cocultures. Cocultures were inoculated with *E. coli* and *R.*
514 *palustris* at equivalent cell densities with excess carbon available for both species (25 mM glucose for *E.*
515 *coli* and 20 mM sodium acetate for *R. palustris*). NH_4^+ was added to cocultures to a final concentration of
516 0.5 μM every hour for 96 hours. The dotted line indicates a competitive index value of 1, where both
517 species are equally competitive for NH_4^+. Filled triangles, WT *E. coli*; open triangles *E. coli* ΔAmtB.
518 Error bars indicate SD, n=3. Different letters indicate statistical differences between *E. coli* competitive
519 index values, $p < 0.05$, determined by one-way ANOVA with Tukey's multiple comparisons post test.

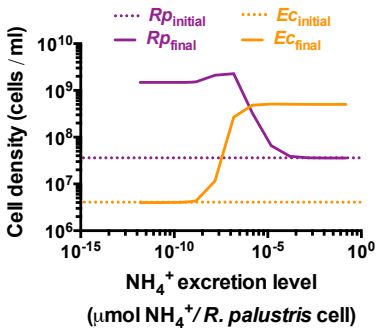

Fig. 6. Higher *R. palustris* NH_4^+ excretion levels are predicted to compensate for a low *E. coli* NH_4^+ affinity. 300 h batch cultures were simulated with a relative *R. palustris* : *E. coli* (*Ec* : *Rp*) K_M value for NH_4^+ of 0.001 over different *R. palustris* NH_4^+ excretion levels (R_A). Final cell densities, solid lines; initial cell densities, dotted lines.

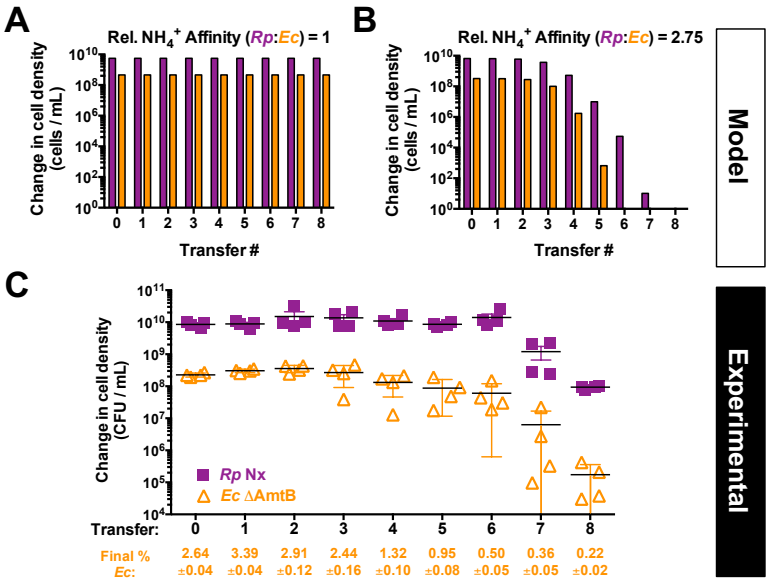

Fig. 7. A low *E. coli* NH_4^+ affinity results in coculture collapse over serial transfers when paired with *R. palustris* Nx. (**A**,**B**) 300 h batch cultures were simulated and serial transferred used a 1% inoculum based on the cell density at 300 h for the previous culture. Relative NH_4^+ affinity values represent the relative *E. coli* K_M for NH_4^+ (K_A) compared to that of *R. palustris* (K_{AR}). (**C**) Final cell densities of *R. palustris* Nx and *E. coli* ΔAmtB of cocultures grown for one week, less than 24 hours into stationary phase. A 1% inoculum was used for each subsequent serial transfer. Error bars indicate SD, n=4. Final *E. coli* cell percentages +/- SD for each transfer are shown.

Recipient-biased competition for a cross-fed nutrient is required for coexistence of microbial mutualists

Alexandra L. McCully, Breah LaSarre, James B. McKinlay[#]

Supplementary Materials.

SyFFoN_v3 description.

Equations 1 – 4 were used to describe *E. coli* and *R. palustris* growth rates:

Eq. 1: *E. coli* growth rate; $\boldsymbol{\mu_{Ec}} = \mu_{EcMAX}\bullet[G/(K_G+G)]\bullet[A/(K_A+A)]\bullet[b_{Ec}/(b_{Ec}+10^{(f+C)})]$

Eq. 2: *R. palustris* growth rate (N_2); $\boldsymbol{\mu_{Rpn}} = \mu_{RpMAX}\bullet[C/(K_C+C)]\bullet[N/(K_N+N)]\bullet[b_{Rp}/(b_{Rp}+10^{(f+C)})]$

Eq. 3: *R. palustris* growth rate (NH_4^+); $\boldsymbol{\mu_{Rpa}} = \mu_{RpMAX2}\bullet[C/(K_C+C)]\bullet[A/(K_{AR}+A)]\bullet[b_{Rp}/(b_{Rp}+10^{(f+C)})]$

Eq 4: Total *R. palustris* growth rate; $\boldsymbol{\mu_{Rp}} = \mu_{Rpn}+ \mu_{Rpa}$

Equations 5-14 were used to describe temporal changes in cell densities and extracellular compounds. Numerical constants in product excretion equations are used to account for molar stoichiometric conversions. Numerical constants used in sigmoidal functions are based on those values that resulted in simulations resembling empirical trends. All R and r parameters are expressed in terms of glucose consumed except for $R_{A,}$ which is the amount of NH_4^+ produced per *R. palustris* cell (Supplementary Table 1).

Eq. 5: Glucose; $\boldsymbol{dG/dt} = -\mu_{Ec}\bullet Ec/Y_G - \mu_{Ec}\bullet Ec\bullet(R_c+R_f+R_e+R_{CO2}) - Ec\bullet(G/(K_G+G))\bullet(10/(10+1.09^{(1000\bullet\mu Ec)}))\bullet(b_{Ec}/(b_{Ec}+10^{(f+C)}))\bullet((100/(100+6^C))\bullet(r_C+r_f+r_e+r_{CO2}) + r_{C_mono} + r_{f_mono} + r_{e_mono} + r_{CO2_mono})$

Eq. 6: N_2; $\boldsymbol{dN/dt} = -\mu_{Rp}\bullet Rp\bullet 0.5\bullet Ra\bullet(1-(40/(40+1.29^N)) - \mu_{Rp}\bullet Rp/Y_N$

Eq. 7: Consumable organic acids; $\boldsymbol{dC/dt} = Ec\bullet\mu_{Ec}\bullet R_c\bullet 2 + Ec\bullet 2\bullet(G/(K_G+G))\bullet(10/(10+1.09^{(1000\bullet\mu Ec)}))\bullet(b_{Ec}/(b_{Ec}+10^{(f+C)}))\bullet(r_C\bullet(100/(100+6^C))+r_{C_mono}) - (\mu_{Rp}\bullet Rp/Y_C) – 0.25\bullet Rp\bullet\mu_{Rp}\bullet Rh_{Rp} - 0.25\bullet Rp\bullet r_{Hp}\bullet(C/(K_C+C))\bullet(40/(40+1.29^N))\bullet(b_{Rp}/(b_{Rp}+10^{(f+C)}))$

Eq. 8: Formate; $\boldsymbol{df/dt} = (Ec\bullet\mu_{Ec}\bullet R_f\bullet 6) + Ec\bullet 6\bullet(G/(K_G+G))\bullet(10/(10+1.09^{(1000\bullet\mu Ec)}))\bullet(b_{Ec}/(b_{Ec}+10^{(f+C)}))\bullet(r_f\bullet(100/(100+6^C)) + r_{f_mono}$

Eq. 9: NH_4^+; $\boldsymbol{dA/dt} = Rp\bullet\mu_{Rp}\bullet R_A\bullet(1-(40/(40+1.29^N))) - \mu_{Ec}\bullet Ec/Y_A – (\mu_{Rp}\bullet Rp/Y_{AR})\bullet(A/(K_{AR}+A))$

Eq. 10: *E. coli*; $\boldsymbol{dEc/dt} = \mu_{Ec}\bullet Ec$

Eq. 11: *R. palustris*; $\boldsymbol{dRp/dt} = \mu_{Rp}\bullet Rp$

575
576 Eq. 12: Ethanol; $\boldsymbol{de/dt} = Ec \bullet 3 \bullet (\mu_{Ec} \bullet R_e + (G/(K_G+G)) \bullet (10/(10+1.09^{(1000 \bullet \mu Ec)}))$
577 $\bullet (b_{Ec}/(b_{Ec}+10^{(f+C)})) \bullet (r_e \bullet (100/(100+6^C)) + r_{e_mono}))$
578
579 Eq. 13: CO_2; $\boldsymbol{dCO2/dt} = Ec \bullet 6 \bullet (\mu_{Ec} \bullet R_{CO2} + (G/(K_G+G)) \bullet (10/(10+1.09^{(1000 \bullet \mu Ec)}))$
580 $\bullet (b_{Ec}/(b_{Ec}+10^{(f+C)})) \bullet (r_{co2} \bullet (100/(100+6^C)) + r_{co2_mono}))$
581 $+ Rp \bullet 0.5 \bullet (\mu_{Rp} \bullet Rh_{Rp} + r_{Hp} \bullet (C/(K_C+C)) \bullet (40/(40+1.29^N)) \bullet (b_{Rp}/(b_{Rp}+10^{(f+C)})))$
582 Eq. 14: H_2; $\boldsymbol{dH/dt} = Rp \bullet (\mu_{Rp} \bullet R_{HRp} + r_{Hp} \bullet (C/(K_C+C)) \bullet (40/(40+1.29^N)) \bullet$
583 $(b_{Rp}/(b_{Rp}+10^{(f+C)}))) + Ec \bullet (\mu_{Ec} \bullet R_{HEc} + (G/(K_G+G)) \bullet (10/(10+1.09^{(1000 \bullet \mu Ec)})) \bullet$
584 $(b_{Ec}/(b_{Ec}+10^{(f+C)})) \bullet (r_H \bullet (100/(100+6^C)) + r_{H_mono}))$
585
586 Where,
587 μ is the specific growth rate of the indicated species (h^{-1}).
588
589 μ_{MAX} is the maximum specific growth rate of the indicated species (h^{-1}).
590
591 G, A, C, N, f, e, H and CO2 are the concentrations (mM) of glucose, NH_4^+, consumable organic
592 acids, N_2, formate, ethanol, H_2, and CO_2, respectively. All gasses are assumed to be fully
593 dissolved. Consumable organic acids are those that *R. palustris* can consume, namely, lactate (3
594 carbons), acetate (2 carbons), and succinate (4 carbons). All consumable organic acids were
595 simulated to have three carbons for convenience. Only net accumulation of formate, ethanol,
596 CO_2 and H_2 are described in accordance with observed trends.
597
598 K is the half saturation constant for the indicated substrate (mM).
599
600 Ec and Rp are the cell densities (cells/ml) of *E. coli* and *R. palustris*, respectively.
601
602 b is the ability of a species to resist the inhibiting effects of acid (mM).
603
604 Y is the *E. coli* or *R. palustris* cell yield from the indicated substrate (cells / μmol glucose). Y
605 values were determined in MDC with the indicated substrate as the limiting nutrient.
606
607 R is the fraction of glucose converted into the indicated compound per *E. coli* cell during growth
608 (μmol of glucose / *E. coli* cell), except for R_A. Values were adjusted to accurately simulate
609 product yields measured in cocultures and in MDC with and without added NH_4Cl.
610
611 R_A is the ratio of NH_4^+ produced per *R. palustris* cell during growth (μmol / *R. palustris* cell).
612 The default value was based on that which accurately simulated empirical trends.
613 r is the growth-independent rate of glucose converted into the indicated compound (μmol / cell /
614 h). Default values are based on those which accurately simulated empirical trends in coculture.
615
616 $r_{_mono}$ is the growth-independent rate of glucose converted into the indicated compound by *E. coli*
617 when consumable organic acids accumulate. Default values are based on linear regression of
618 products accumulated over time in nitrogen-free cell suspensions of *E. coli* (26).

619 **Supplementary Table 1. Default parameter values used in the model unless stated otherwise**
620

Parameter	Value	Description (Units); Source
μ_{EcMAX}	0.2800	*E. coli* max growth rate (h^{-1}); Monoculture
μ_{RpMAX}	0.0772	*R. palustris* max growth rate (h^{-1}); Monoculture
μ_{RpMAX2}	0.0152	Boost on *R. palustris* growth rate in presence of NH_4^+ (h^{-1}); Monoculture[a]
G	25	Glucose (mM)
A	0.00005	NH_4^+ (mM); from initial $(NH_4)_6Mo_7O_{24}\cdot 4H_2O$ concentration
C	0	Consumable organic acids (those that *R. palustris* was observed to consume: lactate, acetate, and succinate; mM)
N	70	N_2 (assumed to be fully dissolved; mM)
f	0	Formate (mM)
e	0	Ethanol (mM)
CO2	0	Carbon dioxide (mM)
K_G	0.02	*E. coli* affinity (Michaelis-Menten constant (K_M)) for glucose (mM); (57)
K_C	0.01	*R. palustris* affinity (K_M) for consumable organic acids (mM); Assumed
K_A	0.01	*E. coli* affinity for NH_4^+ (mM); (58)
K_{AR}	0.01	*R. palustris* affinity for NH_4^+ (mM); Assumed[b]
K_N	6	*R. palustris* affinity (K_M) for N_2 (mM)
Ec	0.4×10^7	*E. coli* cell density (cells / ml)
Rp	3.6×10^7	*R. palustris* cell density (cells / ml)
b_{Ec}	10^{43}	Resistance of *E. coli* to low pH (mM)
b_{Rp}	10^{32}	Resistance of *R. palustris* to low pH (mM)
Y_G	8×10^7	Glucose-limited *E. coli* growth yield (cells / µmol glucose); Glucose-limited *E. coli* culture
Y_A	1×10^9	NH_4^+-limited *E. coli* growth yield (cells / µmol NH_4^+); NH_4^+-limited *E. coli* culture
Y_C	2.5×10^8	Organic acid-limited *R. palustris* growth yield (cells / µmol organic acid); Acetate-limited *R. palustris* culture
Y_N	5×10^8	N_2-limited *R. palustris* growth yield cells / µmol N_2; N_2-limited *R. palustris* culture
R_C	1.9×10^{-8}	Fraction of glucose converted to organic acids (µmol glucose / cell)
R_f	8×10^{-9}	Fraction of glucose converted to formate (µmol glucose / cell)
R_e	4.5×10^{-9}	Fraction of glucose converted to ethanol (µmol glucose / cell)
R_{CO2}	5×10^{-10}	Fraction of glucose converted to CO_2 (µmol glucose / cell)
R_{HRp}	2×10^{-9}	*R. palustris* H_2 production (µmol H_2 / *R. palustris* cell)
R_{HEc}	5×10^{-9}	*E. coli* H_2 production (µmol H_2 / *E. coli* cell)
R_A	0.15×10^{-9}	*R. palustris* NH_4^+ production (µmol NH_4^+ / cell)
r_C	300×10^{-11}	*E. coli* specific growth-independent rate of glucose conversion to consumable organic acids (µmol glucose / cell / h) (33)
r_f	47×10^{-11}	*E. coli* specific growth-independent rate of glucose conversion to formate (µmol glucose / cell / h) (33)
r_e	15×10^{-11}	*E. coli* specific growth-independent rate of glucose conversion to ethanol (µmol glucose / cell / h) (33)
r_{CO2}	2×10^{-11}	*E. coli* specific growth-independent rate of glucose conversion to CO_2 (µmol glucose / cell / h) (33)m
r_H	2×10^{-11}	*E. coli* specific growth-independent rate of H_2 production (µmol H_2 / cell / h) (33)
r_{C_mono}	1.2×10^{-11}	*E. coli* specific growth-independent rate of glucose conversion to consumable organic acids when consumable organic acids accumulate (µmol glucose / cell / h); (26)
r_{f_mono}	0.83×10^{-11}	*E. coli* specific growth-independent rate of glucose conversion to formate when consumable organic acids accumulate (µmol glucose / cell / h); (26)
r_{e_mono}	0.5×10^{-11}	*E. coli* specific growth-independent rate of glucose conversion to ethanol

		when consumable organic acids accumulate (μmol glucose / cell / h); (26)
r_{co2_mono}	1.3×10^{-11}	*E. coli* specific growth-independent rate of glucose conversion to CO_2 when consumable organic acids accumulate (μmol glucose / cell / h); (26)
r_{H_mono}	0.83×10^{-11}	*E. coli* specific growth-independent rate of glucose conversion to H_2 when consumable organic acids accumulate (μmol glucose / cell / h); (26)
r_{Hp}	27×10^{-11}	*R. palustris* specific growth-independent rate of H_2 production (μmol H_2 / cell / h)

621 [a] Increased growth rate in presence of NH_4^+ versus N_2 based on the difference in experimentally
622 determined growth rates in *R. palustris* monocultures grown with either NH_4^+ or N_2 as a nitrogen
623 source.
624 [b] K_{AR} was assumed to be equivalent to the published *E. coli* K_M (58) for NH_4^+ (K_A).
625
626
627
628 **Supplementary Table 2. Strains, plasmids, and primers used in this study.**
629

Strain or plasmid	**Description or Sequence (5'-3'); Designation**	**Source or Purpose**
***R. palustris* strains**		
CGA009	Wild-type strain; spontaneous Cm^R derivative of CGA001	(51)
CGA4004	CGA009 Δ*hupS* Δ*rpa2750*; Parent	(26)
CGA4005	CGA4004 *nifA**; Nx	(26)
CGA4021	CGA4005 Δ*amtB1* Δ*amtB2* ; Nx ΔAmtB	(26)
CGA4026	CGA4004 Δ*amtB1* Δ*amtB2;* ΔAmtB1,	This study
***E. coli* strains**		
MG1655	Wild-type K12 strain, WT	(59)
K-12 JW0441-1	Keio collection Δ*amtB::Km*	(54)
MG1655ΔAmtB	MG1655 Δ*amtB::Km*; ΔAmtB	This study
Plasmids		
pJQnifA16	Gm^R; WT *nifA* gene flanked by XbaI/BamHI cloned into pJQ200SK	This study
Primers		
ALM6f	TTCGTCGCTGAATTGCAACG	*amtB* upstream flanking region (*E. coli*)
ALM6r	TCAGGAAGGGGTGATGCGTA	*amtB* downstream flanking region (*E. coli*)
JBM1	CGTCTAGACCGGCGCATCGC	*nifA16* upstream primer; XbaI
JBM6	GGGGATCCTGGTTCGCAGAGG	*nifA16* downstream primer; BamHI

630

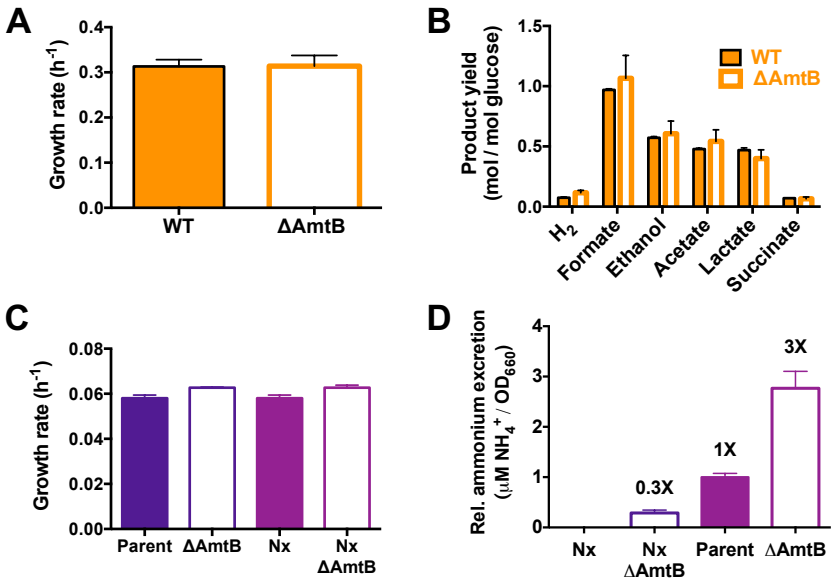

Supplementary Fig. 1. *E. coli* ΔAmtB and *R. palustris* ΔAmtB monoculture growth and metabolic trends. (**A**,**B**) Growth rates (**A**) and fermentation product yields (**B**) from WT *E. coli* (filled) or without (open) *E. coli* ΔAmtB monocultures grown in MDC with 25 mM glucose and 15 mM NH_4Cl. Fermentation profiles were generated from stationary monocultures. Error bars indicate SD, n=3. (**C**,**D**) Growth curves (**C**) and relative NH_4^+ excretion (**D**) of *R. palustris* monocultures grown in MDC with 3 mM sodium acetate and a 100% N_2 headspace. Error bars indicate SD, n=4

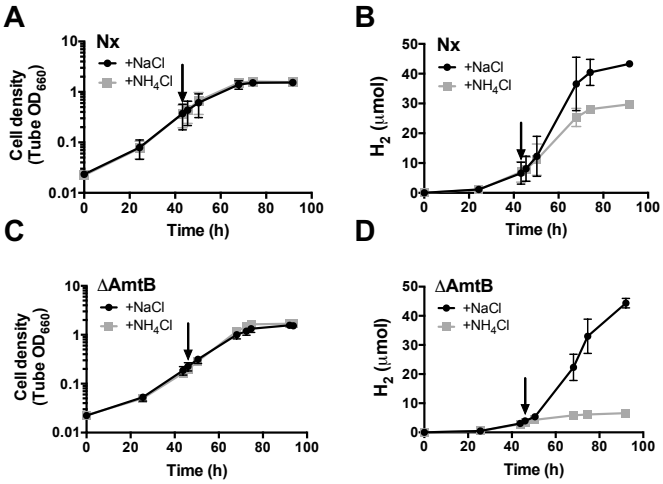

Supplementary Fig. 2. *R. palustris* ΔAmtB responds to NH_4^+-induced shutoff of nitrogenase. The effect of either NH_4Cl or NaCl on growth (**A**,**C**) and H_2 production (**B**,**D**) in *R. palustris* Nx or *R. palustris* ΔAmtB monocultures. *R. palustris* monocultures were grown in MDC with 20 mM sodium acetate and a 100% N_2 headspace until mid-exponential phase and then supplemented with either 15 mM NH_4Cl or 15 mM NaCl at the time indicated by the arrow.

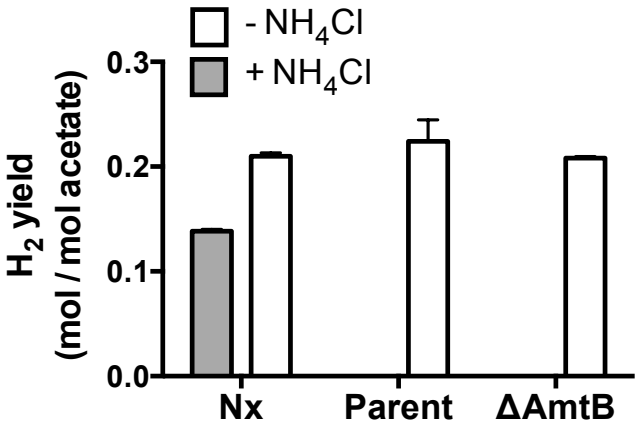

Supplementary Fig. 3. Unlike *R. palustris* Nx, *R. palustris* ΔAmtB does not produce H_2 when grown with NH_4^+. *R. palustris* monocultures were grown in MDC with 20 mM sodium acetate and a 100% N_2 headspace with (grey) or without (white) 15mM NH_4Cl. Samples for determining H_2 yields were taken one week after inoculation, within 24 hours into stationary phase. Error bars indicate SD, n=3.

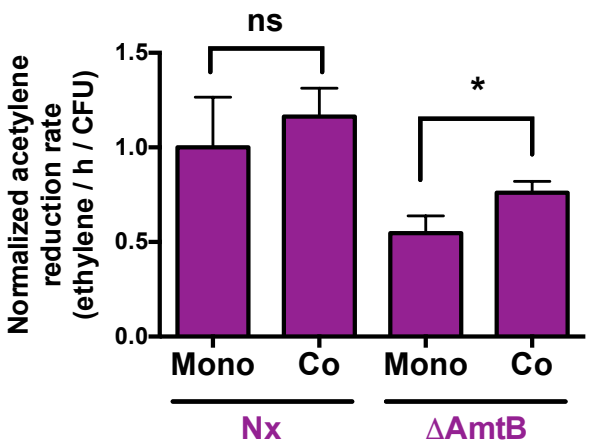

Supplementary Fig. 4. *R. palustris* ΔAmtB nitrogenase activity increases in coculture. Normalized nitrogenase activity of *R. palustris* in monoculture (Mono) or coculture (Co) measured by an acetylene reduction assay. Ethylene levels were divided by total *R. palustris* CFUs in the test tube and then normalized to the *R. palustris* Nx monoculture value. Error bars indicate SD, n=4. *, statistical difference between monoculture and coculture conditions, $p < 0.05$, determined using multiple two-tailed t-tests; ns, no significant difference.